Simulated measurements and imaging of methane emissions at paddock scales.

Stephen W. Wood[1] (s.wood@niwa.co.nz), S. W. Wood, J. B. Liley and P. V Johnston

National Institute of Water & Atmospheric Research, Lauder, P. Bag 50061, Omakau, Central Otago

Introduction

Much of the work on methane emissions in this country has been at the scale of individual animals. Some work a paddock scales has been done using spectrometric techniques. Remote sensing instruments to detect, and in some cases image, gas leaks are now available. Figures R1 and R2 show some examples.

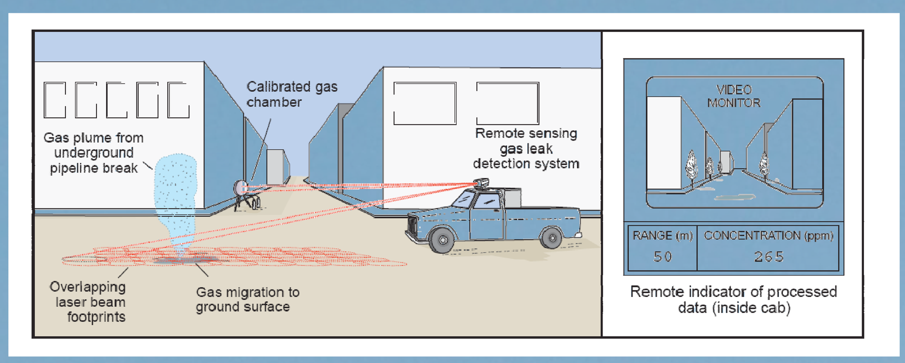

Figure R1. Diagram illustrating the operation of a vehicle mounted gas leak detection system.

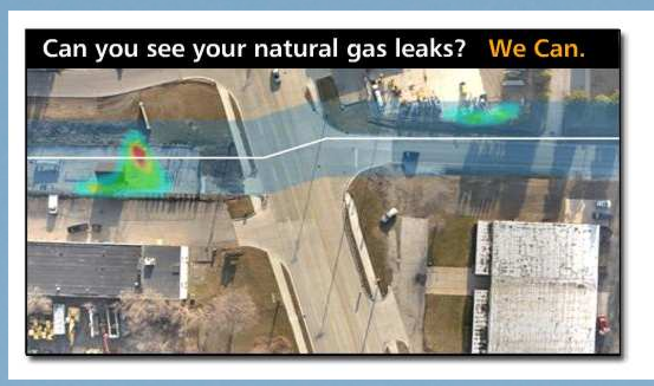

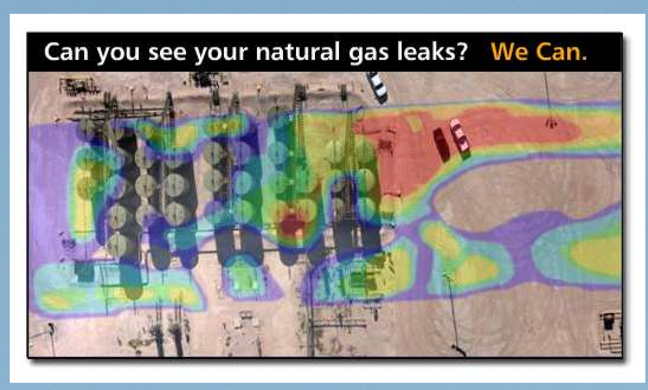

Figure R2. Two examples of gas imaging from an airborne gas detection system overlaid on photos of the area scanned.

In both these examples, the signal reflected from the scene itself is being used for detection. Here we explore whether such a system could be used in a farm setting to observe animal emissions. Our study consists of two parts; a concept design of a suitable instrument, and some simulations of what it might see in a representative farm situation.

Concept design with precision estimates for a Tuneable Diode Laser Absorption Spectrometer (TDLAS) for paddock column CH_4 measurements

To estimate the sensitivity of using long path spectroscopic measurements in paddock scale studies of methane emissions from animals, a Tuneable Diode Laser Absorption Spectrometer (TDLAS) design was investigated. The precision of such measurements has been estimated for a system built with off-the-shelf optical components. We estimate the precision of a column measurement using the paddock itself as the reflector; what might be called a 'paddock path'. Analogous to the gas leak imaging above, such a system could scan the target area. We consider how accurate a 2-D image of the area using tomography or other inversion techniques will be.

System

The design uses a commercial Tuneable Diode Laser (TDL) operating in the 1.65 µm region mounted on or close to a coaxial telescope with the laser light propagated outwards from the centre of the telescope. The returned light is collected by the telescope and focused onto a cooled InGaAs photodiode detector. A telescope of diameter 100 mm (4 inches) would be compact enough to enable scanning of a target area. This combination is the TDLAS instrument.

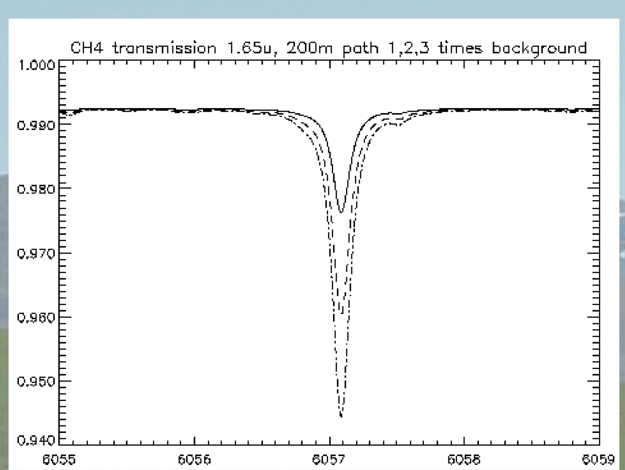

Figure C1 The 1.65µm CH_4 absorption line for simulated conditions.

CH_4 Absorption

Figure C1 shows the results of transmission calculations of 1, 2 and 3 times background concentrations of CH_4 for a reflection distance of 100 m and a temperature of 290 K, chosen as typical of farm scale measurements. The optical path is twice the path from the TDLAS telescope to the point on the paddock where the laser light is reflected, or scattered, back toward the telescope.

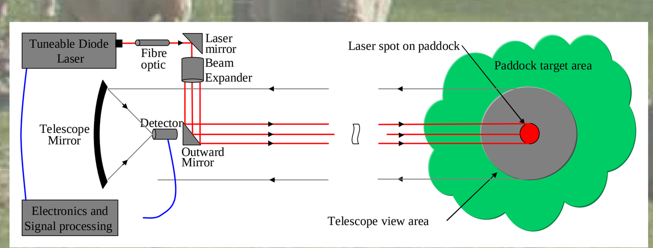

Figure C2 The TDLAS and paddock target area optical geometry. The telescope mirror has the photodiode detector on its optical axis at the focal length of the mirror (so focused at infinity). On the back of the detector is a 45º mirror which sends the beam-expanded laser light out along the optical axis of the spectrometer.

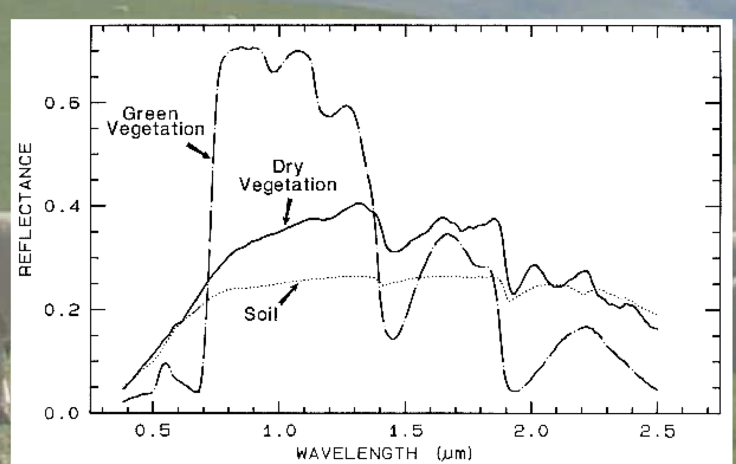

Figure C3 Reflectance spectra of photosynthetic (green) vegetation, non-photosynthetic (dry) vegetation, and a soil. The green vegetation has absorptions short of 1 µm due to chlorophyll. Those at wavelengths greater than 0.9 µm are dominated by liquid water. The dry vegetation shows absorptions dominated by cellulose, but also lignin and nitrogen. These absorptions must also be present in the green vegetation, but can be detected only weakly in the presence the stronger water bands. The soil spectrum shows a weak signature at 2.2 µm due to montmorillonite. Source: USGS web page.

Calculations of the sensitivity and performance that could be expected of such a TDLAS system, taking into account laser power, optics, reflectance of vegetation and soil at 1.65 µm (see Figure C3), detector sensitivity, and sources of noise, show that for a 1 second measurement of the absorption (from two 0.5 s intensity measurements) the resulting error in calculated CH_4 is ~4%. Longer times would reduce the error but limit scanning ability.

We conclude that, in principle, existing technology could be used to construct a 100 mm TDLAS instrument to measure the total column CH_4 amount over a 100 m path to a reflection point in a paddock with a 1-σ accuracy of about 4% for a 1 second measurement time. The effects of atmospheric turbulence and paddock reflectivity variations with incident angle would need to be considered in greater depth before embarking on building an evaluation system.

Simulated observations for a steerable 'paddock path' methane lidar

The simulations are based on a simple Gaussian plume model of methane dispersion from grazing ruminants. More detailed simulation could be based on modelling the hydrodynamic flow, including buoyancy of the eructed gas, variable terrain, and disturbance of the flow by features, surface roughness, and the animals themselves. We assume level terrain in an open rural area.

We adopt a wind speed of 1 m s^{-1}, and atmospheric stability class C on Pasquill's scale, giving neutral density typical of the daytime boundary layer over pasture. We further assume constant emission rates, consistent with the stack gas dispersion model. Representative annual emissions of 12, 70, and 100 kg of methane respectively for sheep, beef cattle, and dairy cows equate to instantaneous rates of 0.38, 2.2, and 3.2 mg s^{-1}.

In the figures below we envisage seven beef cattle, all with equal constant emissions, in a flat paddock that is viewed from above in Figure S1. The scales are in metres down wind and across the plume, with grid step of 0.5 m horizontally and 0.25 m in the (unseen) vertical dimension to allow for slower vertical dispersion. Shaded contours in S1 show just emissions from the animals, and the shading is arbitrary at this stage.

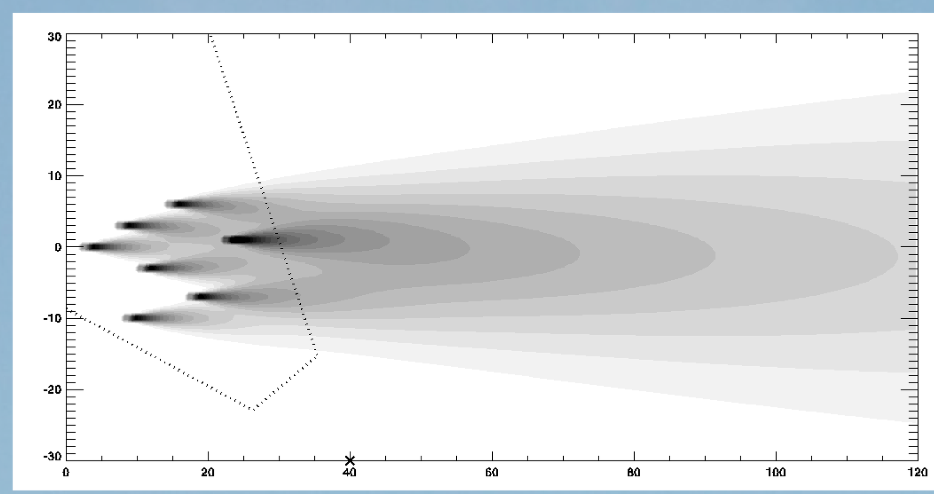

Figure S1. Simulated emission from seven animals in a flat paddock, with 1 m s^{-1} constant wind flow from left to right, neutral air stability, and constant emission rate. The viewpoint and field of view for subsequent figures are shown.

From the viewpoint marked with an **x**, and field of view as shown, the plume would appear as in Figure S2. This image assumes an imaging grid in unit percentage steps of angle, corresponding for example to 1 cm steps across a screen at 1 m. Such high resolution imaging would be difficult to achieve with low measurement frequency (long accumulation time) if the scene is changing, but plausible for this stationary plume.

One characteristic to note is that although all sources are of equal strength, they appear to vary because of differences in where the measurement laser beam passes through the plume in the region of very steep concentration gradients close to the source. This is a recurrence of the point-sampling problem – if you sample where the signal is strongest, small differences in location give large differences in measurement.

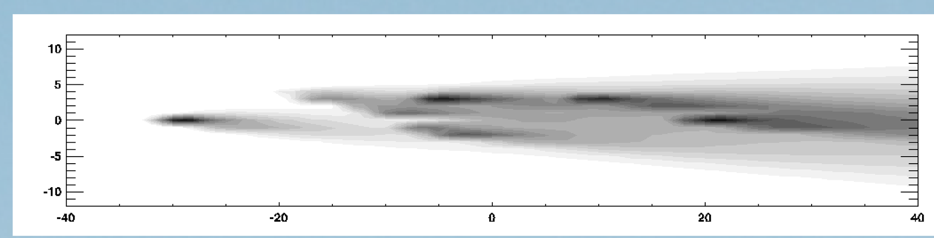

Figure S2. Simulated emissions as in Figure S1, from the viewpoint shown at 5 m elevation.

The density scale in Figure S2 is exaggerated; at 1651 nm absorption in this plume would be less than 1%, but a small absorption signal is no problem if the noise is sufficiently low. The bigger concern is the effect of background methane concentrations, which we take to be 1750 (mean) ± 10 (normal s.d.) ppb. Adding this background gives the image shown in Figure S3

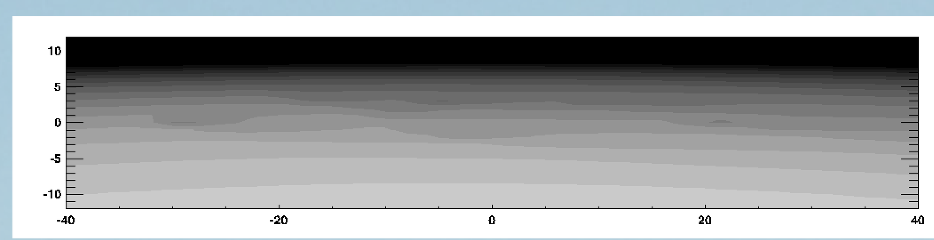

Figure S3. As in Figure S2, but with background concentration added. Contours are in steps of the calculated detection limit for the 1651 nm system discussed in the text.

Although the presence of emission sources is still visible, they are much less apparent. The importance of detector noise is even more apparent when we add a Gaussian component of this order into the image, as in Figure S4.

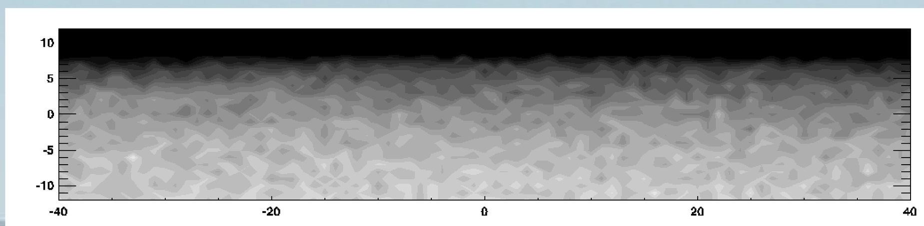

Figure S4. As in Figure S3, with the addition of detector noise for the 1651 nm system.

The 1651 nm system was based on a diode laser run in continuous mode, rather than pulsed, so it cannot be used for ranging in the lidar sense (time delay of returned signal). Nevertheless it is straightforward to do this with a separate pulsed source, so that the path length can be found for each pixel. Dividing this out of the image gives the average concentration along each path shown in Figure S5.

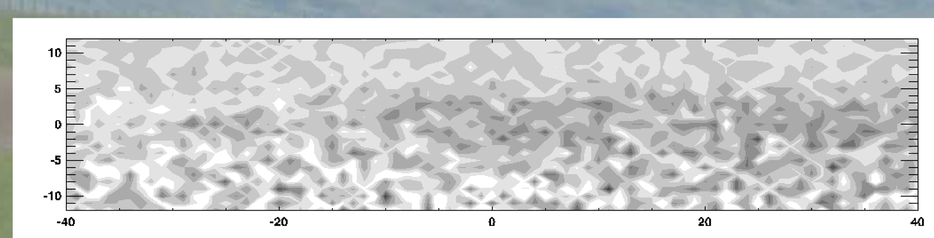

Figure S5. Mean concentration along each sampling path.

Though it only vaguely suggests the outline of the plume from Figure S2, this image at least shows the value of trying to remove the background.

Recognising the importance of detector noise, we envisage a system with 1/8 of the noise level used above. This may be possible with improved detectors, or with a system based on a 3.3 µm. However it might be achieved, an eight-fold improvement in signal-to-noise ratio gives an image as in Figure S6.

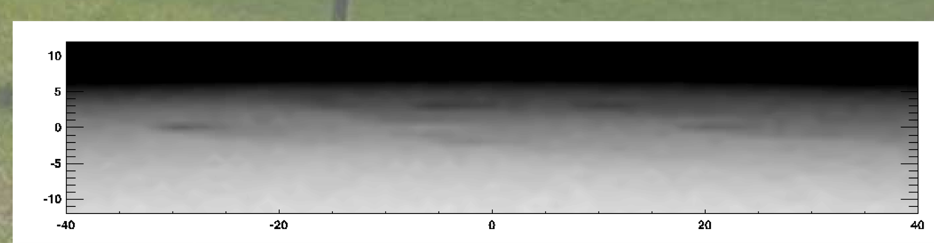

Figure S6. As in Figure S4. but with 8-fold reduction in noise. Contours are adjusted accordingly.

At last in Figure S7 we can again see the plumes shown in Figure S2, endorsing the idea that a steerable lidar system may be able to give useful information about the advection of ruminant methane emissions.

One further problem with the above simulations is the assumption of constant and continuous emission. Keith Lassey (pers. comm.) suggested that perhaps eructions of bubbles of gas at intervals of 1 minute or so would be a more realistic scenario. This would give greater absorption but more spatial variability, and even stronger argument for imaging capability.

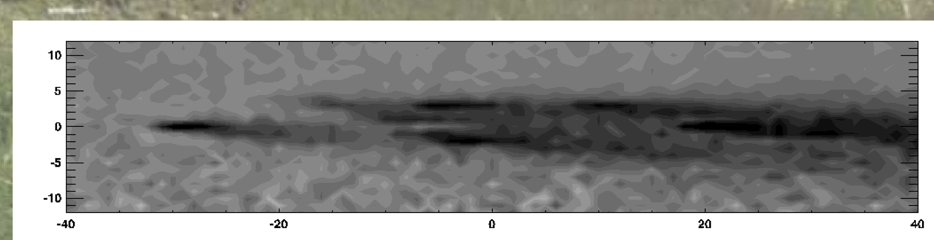

Figure S7. As in Figure S6, expressed as mean concentration in the manner of Figure S5.

NIWA
Taihoro Nukurangi